Hydrogenolysis of Glycidol as an Alternative Route to Obtain 1,3-Propanediol Selectively Using MO_x-Modified Nickel-Copper Catalysts Supported on Acid Mesoporous Saponite

Fiseha B. Gebrestadik,[a] Jordi Llorca,[b] Pilar Salagre,*[a] and Yolanda Cesteros[a]

[a] Dr. F. B. Gebrestadik, Dr. P. Salagre, Dr. Y. Cesteros. Dpt. Quimica Fisica i Inorganica Universitat Rovira i Virgili. C/Marcel·lí Domingo s/n, 43007 Tarragona (Spain) E-mail: pilar.salagre@urv.cat

[b] Dr. J. Llorca. Institut de Tècniques Energètique. Universitat Politècnica de Catalunya. Avda. Diagonal, 647, 08028 Barcelona (Spain)

Abstract

Ni and Cu mono- and bimetallic catalysts modified with various types of acid oxides MOx (M=Mo, V, W, and Re) were tested for the hydrogenolysis of glycidol as an alternative route to the hydrogenolysis of glycerol to obtain 1,3-propanediol (1,3-PrD). Characterization results revealed that the presence of modifiers affected the dispersion and reducibility of the NiO particles and the strength and amount of acid sites. Among the modifiers tested, Re led to the highest activity, a high propanediols selectivity, and the highest 1,3-PrD/1,2-propanediol (1,2-PrD) ratio. The Ni-Cu/Re ratio was optimized to improve the catalytic activity. The best catalytic result, with a 46% 1,3-PrD yield and a 1,3-PrD/1,2-PrD ratio of 1.24, was obtained if the monometallic Ni catalyst at 40 wt% loading and modified with 7 wt% Re was used at 393 K and 5 MPa H2 pressure after 4 h of reaction. The overall 1,3-PrD yield starting from glycerol and assuming a two-step synthesis (glycerol! glycidol!1,3-PrD) and a yield of 78% for the first step would be 36%. This 1,3-PD yield is the highest for a reaction catalyzed by a non-noble metal and is comparable to the direct hydrogenolysis of glycerol using noble metal catalysts at a longer time and a high H2 pressure.

Introduction

Biomass is a renewable source of organic carbon that is becoming important for the production of sustainable fuels and chemicals.[1] One of the most abundant biomass-related renewable materials is glycerol, which is generated during biodiesel production by the transesterification of vegetable oils.[2] Biomass a has higher O/C ratio than most valuable chemicals.[3] Hence, it is desirable to develop catalytic hydrogenolysis reactions to transform it into useful chemical products.[4] Hydrogenolysis catalysts should have the ability to activate hydrogen. Hydrogen can be activated on a metal surface. Typical metals used in hydrogenolysis include Ni, Cu, and noble metals.[4c,5]

The hydrogenolysis of glycerol has been studied widely. With most of the catalytic systems, the main product obtained was 1,2-propanediol (1,2-PrD).[6] However, the hydrogenolysis of glycerol to 1,3-propanediol (1,3-PrD) is economically more attractive because 1,3-PrD is an important monomer in the synthesis of polypropylene terephthalate (PPT), a polymer that displays excellent properties.[7] Additionally, the current industrial production of 1,3-PrD is costly and involves the use of petrochemical-based hazardous starting materials.[8] In a recent review by Nakagawa et al., W-based materials or acid oxides, such as ReO_x or MoO_x, which are able to activate glycerol were used as cocatalysts of several supported noble metal catalysts to favor the formation of 1,3-PrD.[5b]

With respect to the use of W compounds, the presence of H_2WO_4, phosphotungstic acid ($H_3PW_{12}O_{40}$), silicotungstic acid ($H_4SiW_{12}O_{40}$), or WO_3 in the catalysts favored the selectivity to 1,3-PrD.[9] This has been related to an increase of the amount of Brønsted acid sites in these catalysts.[10] The best result was obtained with a Pt-WO_x/Al_2O_3 catalyst that resulted in a selectivity to 1,3-PrD of 66% for a 64% of conversion at 433 K and 5 MPa H_2 pressure.[5b]

The role of ReO_x to improve the selectivity to 1,3-PrD is associated with the acidity of the @OH groups present on its surface, which are able to activate glycerol.[11] Ir-ReO_x/SiO_2[12] and Rh-ReO_x/SiO_2[13] catalysts were tested for the hydrogenolysis of glycerol at 393 K in the presence of small amounts of mineral or solid acid additives. With Ir-ReO_x/SiO_2, 1,3-PrD was obtained in 46% selectivity at 81% of conversion at 393 K and 8 MPa H_2 after 35 h. Rh-ReO_x/SiO_2 was equally active, but its selectivity to 1,3-PrD was much lower (14%).

In general, the selective hydrogenolysis of glycerol to 1,3PrD requires expensive noble-metal-based catalysts, a high temperature and/or pressure, and long reaction times. Even under these reaction conditions, the yield of 1,3-PrD was low or moderate.[5b] Hence, we propose the use of glycidol as an alternative to glycerol to obtain propanediols by catalytic hydrogenolysis because of the high reactivity of glycidol and because it could be obtained readily from glycerol.[14]

Previously, the hydrogenolysis of tetrahydrofurfuryl alcohol (THFA), a cyclic ether with a similar substitution pattern to glycidol, has been reported using Ir-ReO_x/SiO_2,[15] Rh-ReO_x/ SiO_2,[5b,16] and Rh-MoO_x/SiO_2[17] catalysts. These catalysts led to 1,5-pentanediol (1,5-PD)

with a very high selectivity (>90%). The mechanism of THFA hydrogenolysis involved the adsorption of THFA at the @CH_2OH group on the protonated ReO_x or MoO_x surface. H_2 activated on the metal attacks the C@O bond that neighbors the @CH_2OH substituent and releases 1,5-PD.[15,17a]

In our previous work on the hydrogenolysis of glycidol using catalysts that comprise Ni supported on mesoporous acid saponite (MS), we observed that the presence of strong Brønsted acid sites improved the selectivity to 1,3-PrD.[18] The highest 1,3-PrD/1,2-PrD ratio was 0.97 at total conversion at 453 K using a catalyst with 40 wt% Ni loading. In preliminary studies on the use of bimetallic Ni-Cu catalysts, we found that the NiCu bimetallic catalyst at a Ni/Cu atomic ratio of 6:1 gave a better 1,3-PrD selectivity.

In this work, we modified several MS-supported Ni and Cu mono- and bimetallic catalysts using various MO_x (M=Mo, V, W, and Re) modifiers to investigate their activity for the catalytic hydrogenolysis of glycidol. The effect of the metal to modifier ratio was studied for ReO_x.

Results and Discussion

Characterization of the catalyst precursors and catalysts

XRD patterns of the Ni-Cu and modified Ni-Cu catalyst samples after reduction at 623 K for 6 h are displayed in Figure 1. All catalysts presented peaks at 2q=19.4, 35.6, and 60.58, which correspond to the (110, 020), (201), and (060) reflections of the saponite support, and at 2q=44.5 and 51.98, which are related to the presence of metallic Ni. Broad or shoulder peaks observed in the patterns of Ni-CuMo(7)/MS, Ni-CuV(7)/MS, and Ni-CuW(7)/MS (Figure 1b–d) at 2q=43.2 and 62.88 were identified as the NiO phase. Peaks that correspond to the modifiers or Cu were not observed in any sample, which suggests that they have a small crystallite size or low crystallinity. In addition, there was no appreciable shift in the cell parameters of Ni in the bimetallic catalysts, and the formation of a Ni-Cu alloy was not clear from the XRD pattern. The presence of a modifier seems to favor the dispersion of Ni as the Ni crystallite size decreased from 27 to 11–21 nm in the presence of the modifiers (Table 1). The acidity of the modifiers and the basicity of the NiO phase and the subsequent acid–base interaction could justify this improved dispersion.

Table 1. Characterization results of the catalyst precursors and catalysts.

Catalyst precursor	S_{BET} [$m^2 g^{-1}$]	Average pore radius [Å]	Acidity[a] [$mEq.g^{-1}$]	Acidity[b] [$mEq.g^{-1}$]	Catalyst	Ni (NiO)[c] crystallite size [nm]
PNi-Cu/MS	220	27	0.96	1.02	Ni-Cu/MS	27
PNi-CuV(7)/MS	179	25	1.82	1.85	Ni-CuV(7)/MS	21 (3)
PNi-CuMo(7)/MS	156	26	1.69	1.75	Ni-CuMo(7)/MS	21 (6)
PNi-CuW(7)/MS	157	23	1.74	1.77	Ni-CuW(7)/MS	24 (4)
PNi-CuRe(7)/MS	340	31	1.88	–	Ni-CuRe(7)/MS	11
PNi-CuRe(3)/MS	347	31	1.45	–	Ni-CuRe(3)/MS	12
PNi-CuRe(15)/MS	268	34	1.92	–	Ni-CuRe(15)/MS	14
PNi-Cu*Re(7)/MS	362	30	1.95	2.06	Ni-Cu*Re(7)/MS	6
PNi-Cu**Re(7)/MS	429	33	2.03	2.13	Ni-Cu**Re(7)/MS	3
PNiRe(7)/MS	331	33	1.71	–	NiRe(7)/MS	13

Acidity in $mEq._{CHA}\, g^{-1}$ of sample of the catalyst precursors obtained by using [a] TGA of CHA-treated samples and [b] NH_3-TPD. [c] Average crystallite size obtained by using XRD.

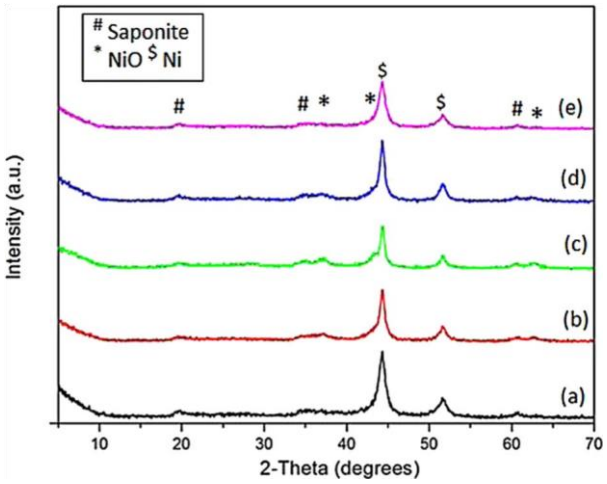

Figure 1. XRD patterns of Ni-Cu/MS samples with 40 wt% Ni-Cu loading a) without modifier and with b) Mo, c) V, d) W, and e) Re modifier at 7 wt% loading.

XRD patterns of supported monometallic Ni and Cu catalysts modified with Re and Ni-Cu bimetallic catalysts with different Ni-Cu loadings [wt%] and different modifier amounts are shown in Figure 2. For the monometallic modified Cu catalyst, sharp peaks were observed at 2q=43.3 and 50.48, which were attributed to a crystalline metallic Cu phase. In the other samples, the Ni phase was mainly observed, and the Ni crystallite size increased with the increase of the Ni-Cu loading. For the catalysts prepared with lower Ni-Cu loadings (30 and 20 wt%; Ni-Cu*Re(7)/MS and Ni-Cu**Re(7)/MS), the peaks appeared broader and a shoulder was observed at approximately 2q= 438, which indicates the presence of residual amounts of NiO. Thermogravimetric analysis (TGA) of cyclohexylamine (CHA) treated modified Ni-Cu catalyst precursors was used to determine the total surface acidity of the samples before reduction (Figure 4). The minima that correspond to the first derivative of the TGA curve can be associated with different processes related to the mass loss. Thus, those centered at approximately 350 and 1100 K can be attributed to the water loss caused by the dehydration of interlayer cations and the dehydroxylation of the saponite structure, respectively. The other minima correspond to the mass loss associated with CHA desorption. The number of these minima can be attributed to different acid sites, and their temperature can be related to their acidity strength. Thus, the minima that appear at a higher temperature correspond to stronger acid sites.

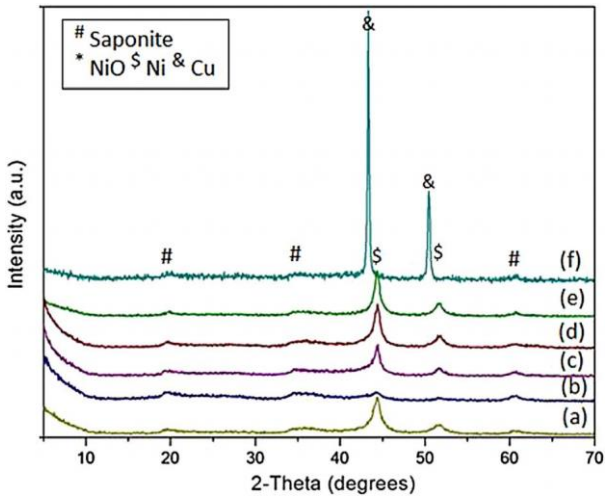

Figure 2. XRD patterns of a) NiRe(7)/MS, b) Ni-CuRe**(7)/MS, c) Ni-Cu*Re(7)/ MS, d) Ni-CuRe(3)/MS, e) Ni-CuRe(15)/MS, and f) CuRe(7)/MS.

For PNi-CuMo(7)/MS, PNi-CuV(7)/MS, and PNi-CuW(7)/MS catalyst precursors, two types of acid sites were observed. The minimum observed for all samples at approximately 600 K was similar to that of the unmodified catalyst precursor. This can be related to the acid sites of the support that were not influenced by the modifiers. Another broader minimum, which appeared at an inflection point of approximately 750 K in these three modified catalyst precursors could be caused by additional stronger acid sites associated with the presence of the modifiers. In contrast, for PNi-CuRe(7)/MS, mainly one minimum at 650 K was observed with only a small shoulder at approximately 600 K. It can be argued that rhenium, nickel, and copper oxides in PNi-CuRe(7)/MS are well dispersed and cover the main part of the support external surface, which favors the interaction of the H^+ of the support with the ReO_x to result in mainly one type of acid site with stronger acidity than that of the support without modifiers. The stronger acid sites detected in the catalyst precursors in the presence of modifiers could be associated with @OH groups[15] or with Lewis acid sites of the modifiers.

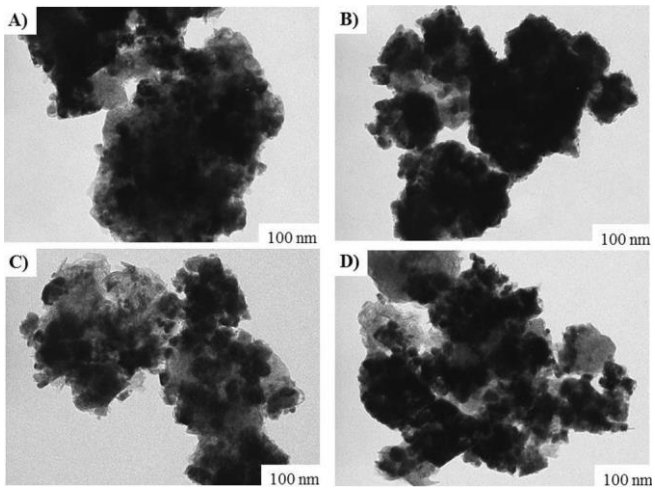

Figure 3. TEM images of A) Ni-Cu/MS, B) Ni-CuMo(7)/MS, C) Ni-CuRe(7)/MS, and D) NiRe (7)/MS at 100 K.

The TGA results of CHA-treated Ni-Cu catalysts precursors at different Ni-Cu loadings and modified with different amounts (Figure 2b and c). The Ni crystallite size in these two samples was 6 and 3 nm, respectively, in agreement with their low metal loading. The value increased to 11 nm for Ni-CuRe(7)/MS. The other samples had comparable crystallite sizes (12–14 nm).

TEM images of Ni-Cu/MS, Ni-CuMo(7)/MS, NiCuRe(7)/MS, and Ni-CuRe(7)/MS (Figure 3A–D, respectively) allowed us to observe that the Ni particles size was similar to that obtained by using XRD.

To explain the XRD results, it is necessary to have information about the interactions between the NiO and CuO phases with the support and the modifiers present in the precursors. Additionally, the acidity of the catalytic precursors could also be an interesting parameter with which to compare the catalysts. For these reasons, acidity and reducibility studies of the catalyst precursors were performed.

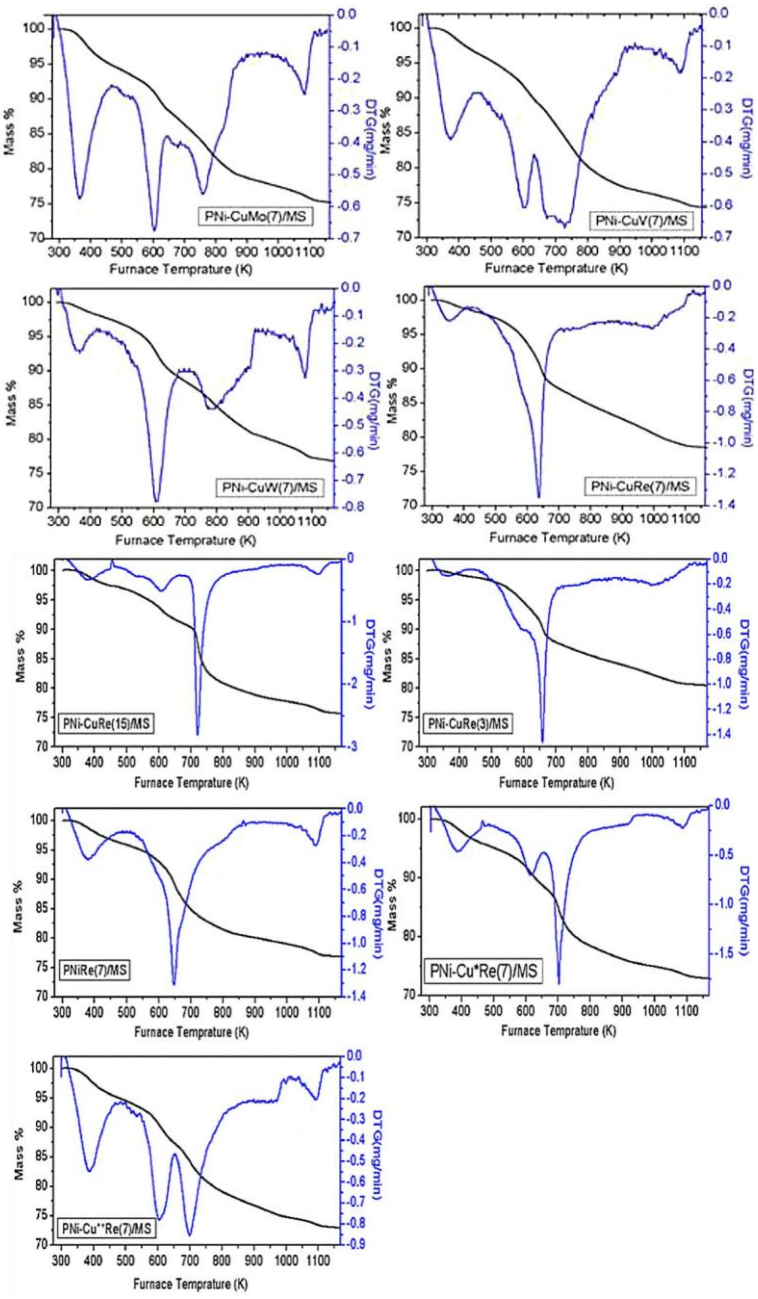

Figure 4. TGA results of CHA-treated samples of the modified catalyst precursors.

Figure 5. TGA results of CHA-treated catalyst precursors with different Re/Ni+Cu ratios.

For all the modified catalyst precursors, except for PNi-CuW(7)/MS, the main reduction peak was shifted to higher temperatures with respect to that of the unmodified one. This shift in the reduction temperature could be related to smaller NiO particles, which interact strongly with the support. This makes the reduction of NiO more difficult. However, the shift for the sample with Re was very small (7 K). This lower shift is difficult to explain, but is probably an opposite effect that takes place in this sample to favor the reduction; this could be caused by a decrease of the electronic density on the Ni^{II} by interaction with the Re_2O_7 phase, which is discussed later. In this sample, additionally, a well-defined peak was observed at a lower reduction temperature (530 K) that could be correlated with more effective of Re are displayed in Figure 5. For catalyst precursors with 40 wt% Ni-Cu loading, the small minimum that corresponds to the loss of CHA adsorbed on the acid sites of the support (600 K), appeared more defined at 3 and 15 wt% Re loading than at 7 wt%. If the Re loading was increased to 15 wt%, the position of the minimum related to the CHA adsorbed on the acid sites generated by the presence of modifiers shifted to a higher temperature (700 K). This minimum also appeared at approximately 700 K for PNi-Cu*Re(7)/MS and PNi-Cu**Re(7)/MS. However, for these two samples, the mass loss because of the desorption of CHA adsorbed on the acid sites that correspond to the support increased if we decreased the Ni-Cu loading. These results are consistent with the lower coverage of the support if the Ni-Cu loading was lower.

The total surface acidity of all the modified catalyst precursors was higher (1.45–2.03 $mEq._{CHA}\,g_{@}^{-1}$) than that of the unmodified Ni-Cu catalyst precursor (0.85 $mEq._{CHA}\,g_{@}^{-1}$; Table 1). This confirms that modifiers provide an additional acidity. The values of total surface acidity increased with an increase in the amount of modifier or a decrease in the Ni-Cu loading.

The temperature-programmed desorption of ammonia (NH_3TPD) was performed for selected catalyst precursor samples (Table 1) to supplement the results obtained by using CHATGA. We observed that the results obtained by using the two methodologies are quite similar, but slightly higher values were obtained by using NH_3-TPD. This is in agreement with the mesoporosity of the saponite support and suggests that there was no accessibility problem to the surface acid sites.

The temperature-programmed reduction (TPR) profiles of the unmodified Ni-Cu catalyst precursors and those modified NiO–Re_2O_7 interactions in some particles.

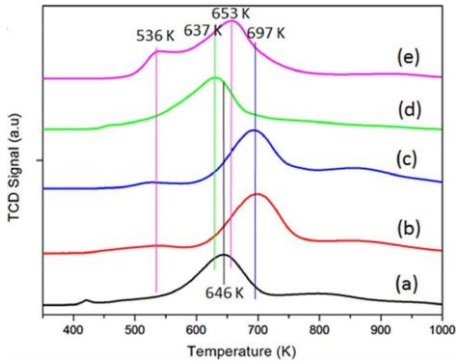

Figure 6. TPR profiles of Ni-Cu/MS catalysts precursors with 40 wt% Ni-Cu loading a) without modifier and b) Mo, c) V, d) W, and e) Re modifier at 7 wt% loading.

For Ni-CuW(7)/MS, the main reduction peak was shifted to a lower temperature by approximately 9 K. In our opinion, this should be more related to a certain decrease of the NiO particle size with respect to that of the unmodified catalyst (from 27 to 24 nm) than to differences in interactions as the degree of NiO dispersion was probably worse if the modifier was WO_3. The larger size of the Ni particles in this catalyst compared with that of the other modified catalysts is in agreement with this. Moreover, this agrees with the fact that this modifier is the oxide with the least acidity in this study.

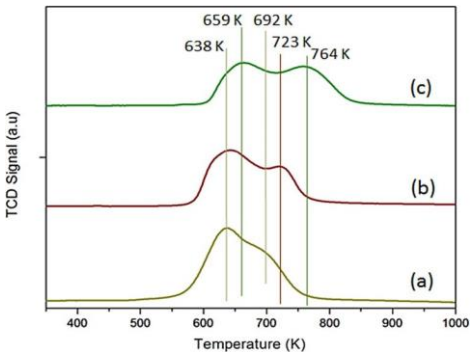

Figure 7. TPR profiles of the catalyst precursors a) PNi(40)Re(7)/MS, b) PNiCu*Re(7)/MS, and c) PNi-Cu**Re(7)/MS.

The reduction profiles of some catalyst precursors with different metal to Re ratios are shown in Figure 7. The reduction of the modified monometallic Ni catalyst precursor, PNiRe(7)/ MS, occurred in a broad interval (570–750 K) with two maxima, one more intense at 639 K and the other at 703 K. If we compare this plot with that of the modified bimetallic catalyst PNiCuRe(7)/MS (Figure 6e), some NiO was reduced easily but the rest was more difficult to reduce. These differences in reducibility could be related to differences in NiO and Re_2O_7 interactions. As mentioned above, an effective NiO–Re_2O_7 interaction should favor NiO reduction.

For the other Ni-Cu catalyst precursors prepared with 20 and 30 wt% total metal loading, the reduction peaks shifted to slightly higher temperatures. Two different reduction peaks were observed for both samples, which might lead to NiO particles with different interactions. The reducibility was more difficult for the precursor that presented the smallest Ni crystallite size (3 nm) after reduction, probably because of a stronger interaction with the support. The reduction peaks at a lower temperature (642 and 659 K for PNi-Cu*Re(7)/MS and PNiCu**Re(7)/MS, respectively) could be attributed to efficient NiO interactions with Re_2O_7 that can favor its reduction. The lower reducibility of these samples could justify the presence of residual amounts of NiO.

The N_2-physisorption analysis results of the catalyst precursors are presented in Table 1. The specific BET areas of all the catalysts precursors were lower than that of the support (600 $m^2 g_{@}^{-1}$),[19] which indicates that some of the pore volume was occupied by metal oxide particles. If we compare the BET areas of the unmodified catalyst precursor with the modified ones, they were lower for the V-, Mo-, and W-modified catalyst precursors. In contrast, for those modified with Re, the BET area was much higher (340 $m^2 g_{@}^{-1}$). This result suggested that Re can favor the dispersion of the metal oxide particles to a greater extent than the other modifiers. The smaller metal crystallite size of the corresponding reduced catalysts, determined by using XRD, could support this, which is discussed later.

At 3 wt% Re loading, the BET area was slightly higher (347 $m^2 g_{@}^{-1}$). However, if the Re loading was increased to 15%, the BET area decreased to 268 $m^2 g_{@}^{-1}$. The BET area of the modified monometallic catalyst precursor, PNiRe(7)/MS (331 $m^2 g_{@}^{-1}$) was slightly lower than that of the bimetallic modified catalyst precursor, PNi-CuRe(7)/MS. This might indicate that the presence of Cu could assist in the dispersion of Ni. The BET area values increased to 362 and 429 $m^2 g_{@}^{-1}$ if the Ni-Cu loading decreased to 30 and 20 wt%, respectively. The average pore radius of all the catalyst precursors was in the mesoporous range (Table 1).

Catalytic activity

Influence of the type of modifier

The catalytic activity involves a complex interplay of competitive and/or cooperative metal and acid sites, as discussed later. For this reason, it was not possible to report catalytic rates in terms of turnover frequencies (TOF). Hence, in this work comparative catalytic activity results are presented based on conversion and selectivity.

The catalytic activity results of Ni-Cu catalysts supported on a mesoporous acid saponite modified with various types of acidic metal oxides are presented in Table 2. The activity should be a result of the combination of the metal and acid sites, responsible for mainly hydrogenolysis and condensation reactions, respectively. These are competitive reactions. However, a cooperative effect of the metal and acid sites could be expected in the hydrogenolysis reaction to result in an increase of the selectivity to 1,3-PrD. This could take place by the activation of glycidol, by the interaction of H^+ with the oxirane ring,[11] or by interactions of acidic metal oxides MO_x with the alcohol functionality of the glycidol.[15]

Table 2. Catalytic activity test results.

Catalyst	Conversion [%]	Selectivity [%]				1,3-PrD/ 1,2-PrD	1,3-PrD yield [%]
		1,2-PrD	1,3-PrD	Propanol	Condensation products (dioxane/dioxolane)		
CuRe(7)/MS	40	9	8	9	59	0.89	3.2
Ni-Cu/MS	73	47	15	5	21	0.33	11.0
Ni-CuMo(7)/MS	73	48	16	7	28	0.33	11.7
Ni-CuV(7)/MS	88	43	19	5	22	0.45	16.7
Ni-CuW(7)/MS	95	66	16	5	2	0.24	15.2
Ni-CuRe(7)/MS	98	45	34	8	8	0.76	31.6
Ni-CuRe(3)/MS	98	49	29	8	14	0.59	28.4
Ni-CuRe(15)/MS	98	42	35	6	13	0.83	34.3
Ni-Cu*Re(7)/MS	96	38	31	8	11	0.82	31.7
Ni-Cu**Re(7)/MS	98	35	31	7	13	0.89	33.3
NiRe(7)/MS	98	38	47	7	6	1.24	46.1
Re(7)/MS	47	n.d.	n.d.	–	59	–	–

The total Ni-Cu loading in * = 30 wt% and ** = 20 wt%, in the other catalysts the total metal loading is 40 wt%. The Ni/Cu molar ratio in the Ni-Cu bimetallic catalysts is 6:1.

All the modified samples showed comparable or higher activities than the unmodified catalyst. This might indicate that the modifiers could have a catalytic role either by acid activation of glycidol in the metal and H^+ cooperative route or as acid catalysts. The diol selectivity of these catalysts increased if W or Re were used as modifiers. This could be explained by the higher amount of metal phase as a consequence of the higher reducibility of the corresponding catalyst precursors. For the Mo- and V-modified catalysts, the propanediols selectivity was lower, in agreement with their lower NiO reducibility and the presence of residual amounts of NiO in the fresh catalysts.

All catalysts displayed a comparable propanol selectivity, which suggests that the formation of propanol was not related to high metal activity and was not the result of the overhydrogenolysis of propanediols. The presence of propanol can be justified by the capacity of Cu to deoxygenate oxirane rings as reported previously.[20] With regard to the condensation product selectivity (dioxane/dioxolane), the unmodified catalyst and those modified with Mo and V gave a comparable selectivity (21–28%). The selectivity towards these products was lower for the Re- and W-modified catalysts. These results agree with the higher metal activity of the Re- and W-modified samples.

With regard to the 1,3-PrD/1,2-PrD ratio, the unmodified catalyst, Ni-Cu/MS, showed a value of 0.33. The value decreased for the W-modified catalyst, was comparable for the Mo-modified catalyst, was slightly higher for the V-modified catalyst, and was higher for the Re-modified catalyst (Table 2). The lower 1,3-PrD/1,2-PrD ratio (0.24) of Ni-CuW(7)/MS could be associated with Ni activity without acid collaboration, probably because of a worse dispersion of WO_3 on the metal particles. For the V- and Re-modified catalysts, the improved 1,3-PrD/1,2PrD ratio might reflect the cooperation between the acid and metal sites. This was especially the case for the Re-modified catalyst. The highest dispersion of the metal and the @OH groups of the ReO_x phase makes this collaborative action possible. In general, among all the modified catalysts tested, the highest 1,3-PrD yield (31.6%) was obtained with Ni-Cu-Re(7)/ MS.

Effect of the Re to metal loading ratio

The effect of the Re loading was studied in two ways; first, the Re loading was varied (3, 7, 15 wt%) at a constant Ni-Cu loading (40 wt%), and second, the Ni-Cu loading was varied (20, 30, and 40%) at a constant Re loading (7 wt%).

The conversion was similar for all catalysts and was not affected significantly by the Re to metal ratio. The selectivity towards each of the products varied depending on the Re/Ni-Cu ratio. If the amount of Re loading increased at a constant NiCu loading, the 1,2-PrD selectivity decreased, the 1,3-PrD selectivity slightly increased, and hence the 1,3-PrD/1,2-PrD ratio increased. This might confirm that ReO_x could be involved in the activation of glycidol to lead to the formation of 1,3-PrD.

All the catalysts gave a comparable propanol selectivity (6– 8%), which suggests that its formation was neither related to acid sites nor to the hydrogenolysis activity of the metal. The selectivity to the condensation products was higher at high and low Re loadings. At a high Re/M molar ratio, this can be related to the higher and stronger acidity (Figure 3), whereas at a low Re loading, it could be associated with lower hydrogenolysis metal activity because of its lower NiO reducibility, as discussed earlier.

If the Ni-Cu loading decreased (40, 30, and 20 wt%), the molar ratio Re/Ni-Cu increased, which resulted in a different catalytic behavior. The propanediols selectivity decreased slightly and the 1,3-PrD/1,2-PrD ratio increased. The selectivity to condensation products increased at a low Ni-Cu loading. The reducibility of NiO was difficult and the acidity was higher for samples with a low metal loading. Hence, the low diol selectivity and high condensation products selectivity could be explained by the low metal and high acid activity, respectively. However, this increase of acidity had a positive effect to improve the selective formation of 1,3-PrD.

Monometallic Re-modified Ni and Cu and the saponite support modified with Re without metal-phase catalysts were prepared (NiRe(7)/MS, CuRe(7)/MS, and Re(7)/MS) and their catalytic activity was tested for comparison (Table 3). The Re-modified Ni catalyst showed the highest selectivity to propanediols (85%) and 1,3-PrD (47%) with the highest 1,3-PrD/1,2-PrD ratio (1.24) and low condensation products selectivity. The high 1,3PrD selectivity could be related to an effective collaborative action between metal and acid sites. However, the modified Cu catalyst afforded the lowest propanediol selectivity, a high propanol selectivity, and the highest condensation products selectivity. This might reflect the poor hydrogenolysis activity of Cu under the conditions used and the high activity of the acid sites. The propanol, as discussed earlier, is the result of Cu-catalyzed deoxygenation of the epoxide ring followed by hydrogenation of the resulting double bond. The Re-modified support showed a comparable moderate activity to that of the modified Cu catalyst with an identical condensation products selectivity. This confirms the previous argument that condensation products can be related to acid sites. The major reaction pathways of the acid- and metal-catalyzed reactions, discussed above, are summarized in Scheme 1.

In summary, among all the modified catalysts tested, the Remodified catalysts showed a higher activity, propanediols selectivity, and 1,3-PrD/1,2-PrD ratio. The experiments on the Re/ M ratio revealed that the optimum modifier and active metal loading was obtained for the monometallic Ni catalyst at 40 wt% loading and with a Re content of 7 wt%. The activity test for this optimum composition, NiRe(7)/MS, at 393 K gave 1,3-PrD in 46.1% yield with a 1,3-PrD/1,2-PrD ratio of 1.24 at 98% of conversion after 4 h of reaction.

Table 3. XPS analysis results of selected fresh, H_2-activated, and spent catalysts.

Catalyst	BE [eV] of characteristic peaks			Re/	Ni/	Ni(Red)/	Cu(Red)/
	Ni	Cu	Re	Ni-Cu	Cu	Ni(Ox)	Cu(Ox)
Re/MS-fresh	–	–	Ox $4d_{5/2}$ 265.1 Red $4d_{5/2}$ 260.8	–	–	–	–
Re/MS- H2 act.	–	–	Ox $4d_{5/2}$ 264.8 Red $4d_{5/2}$ 260.6	–	–	–	–
Ni-CuRe(7)/MS-fresh	Ni^0 $2p_{3/2}$ 852.4 Ni^{2+} $2p_{3/2}$ 854.4	Cu^{2+} $2p_{3/2}$ 933.1 $Cu^{0,+}$ $2p_{3/2}$ 931.1	Ox $4d_{5/2}$ 263.9 Red $4d_{5/2}$ 260.6	0.047	0.15	0.14	1.14
Ni-CuRe(7)/MS- H_2 act.	Ni^0 $2p_{3/2}$ 852.5 Ni^{2+} $2p_{3/2}$ 855.8	Cu^{2+} $2p_{3/2}$ 928.5 $Cu^{0,+}$ $2p_{3/2}$ 931.7	Ox $4d_{5/2}$ 263.5 Red $4d_{5/2}$ 260.6	0.029	0.28	0.15	1.76
Ni-CuRe(7)/MS-spent	Ni^0 $2p_{3/2}$ 852.5 Ni^{2+} $2p_{3/2}$ 854.5	Cu^{2+} $2p_{3/2}$ 932.7 $Cu^{0,+}$ $2p_{3/2}$ 932.2	Ox $4d_{5/2}$ 263.8 Red $4d_{5/2}$ 259.5	0.045	0.19	0.45	3.60
NiRe(7)/MS-fresh	Ni^0 $2p_{3/2}$ 852.6 Ni^{2+} $2p_{3/2}$ 854.7	–	Ox $4d_{5/2}$ 263.4 Red $4d_{5/2}$ 260.0	0.031	–	0.15	–
NiRe(7)/MS- H_2 act.	Ni^0 $2p_{3/2}$ 852.4 Ni^{2+} $2p_{3/2}$ 855.9	–	Ox $4d_{5/2}$ 263.9 Red $4d_{5/2}$ 261.3	0.020	–	0.13	–
NiRe(7)/MS-spent	Ni^0 $2p_{3/2}$ 852.3 Ni^{2+} $2p_{3/2}$ 854.6	–	Ox $4d_{5/2}$ 265.0 Red $4d_{5/2}$ 261.0	0.039	–	0.96	–

The total Ni-Cu loading in * = 30 wt% and ** = 20 wt%, and in the other catalysts the total metal loading is 40 wt%. The Ni/Cu molar ratio in Ni-Cu bimetallic catalysts is 6:1.

Samples were prepared and analyzed by XPS as described in the Experimental Section. The first group of samples was denoted as fresh catalysts as they were the catalysts obtained after reduction and before reaction. However, in these samples some degree of oxidation could be expected during catalyst handling for the XPS analysis. The second group of samples were the catalysts that were activated by reduction in situ with H_2 at 623 K for 30 min, and the third group of samples were the spent catalysts, which were obtained after use in the catalytic test and without any treatment. The support modified with ReO_x without metal, Re/ MS, was also analyzed by using XPS for comparison. The binding energies (BEs) of the characteristic XPS peaks are summarized in Table 3.

The surface composition of the fresh and spent samples was compared to that of the theoretical composition of the catalysts (Table 3). With regard to the ratio between Ni and Cu, the the samples reduced in situ at 623 K had lower Re/metal atomic ratios, Re/Ni=0.020 and Re/(Ni+Cu)=0.029. The decoration of ReO_x by the Ni particles could explain the excellent collaborative effect between Ni and ReO_x in the reaction, which is considered to be responsible for the observed 1,3-PD production with NiRe(7)/MS.

The Re4d spectra of the different catalysts as-prepared (fresh), after in situ H_2 activation at 623 K, and after reaction (spent) are displayed in Figure 8. The spectrum of Re corresponds to the $4d_{5/2}$ peaks as the $4d_{3/2}$ peaks are superposed on the C1s peaks. All the spectra showed two components that correspond to two different oxidation states for Re. The red line indicates the position of the $Re4d_{5/2}$ photoelectrons that correspond to the low oxidation state, and the blue line indicates the position of the $Re4d_{5/2}$ photoelectrons that correspond to the high oxidation state. In the fresh samples, Re was mainly in the high oxidation state for the NiRe(7)/MS and NiCuRe(7)/MS catalysts, whereas in the Re(7)/MS sample the contribution of the less oxidized form was more important. After in situ H_2 activation at 623 K, Re became less oxidized, but there was always a component of highly oxidized Re (probably Re^{VI} or Re^{VII}). Notably, the degree of reduction of Re was similar for Re and NiRe(7)/MS (88–93%), but in Ni-CuRe(7)/MS, Re was much more difficult to reduce (after reduction there was &75% Re reduced to the lower oxidation state). Probably, the Cu–Re interaction favors the electron transfer from Re to Cu, which increases the oxidation state of Re. The spent samples exhibited both Re species in similar amounts as in the corresponding fresh samples.

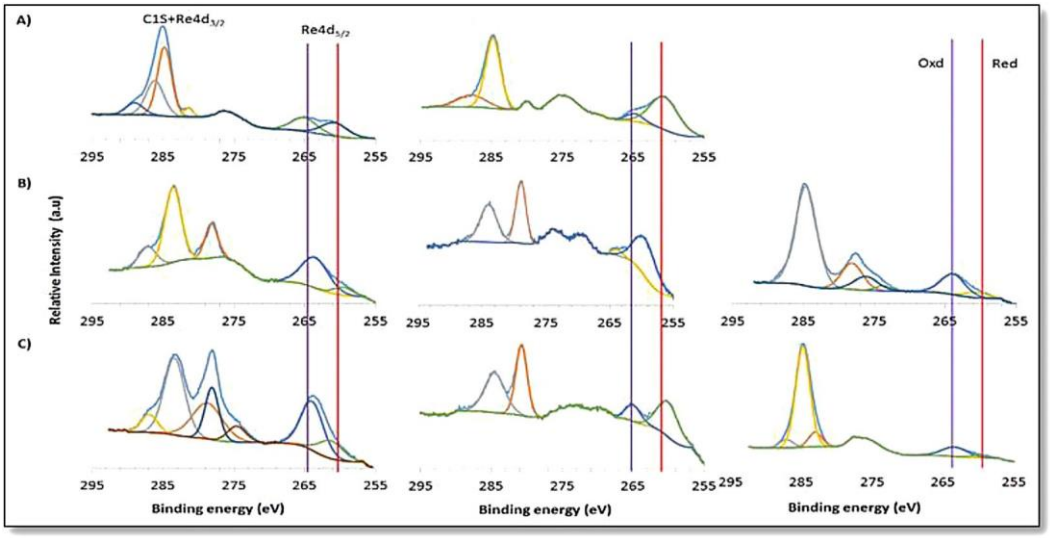

Figure 8. Re4d XPS spectra of A) fresh and H_2-activated Re(7)/MS and fresh, H_2-activated, and spent catalysts from left to right of B) NiRe(7)/MS and C) Ni-CuRe(7)/MS. The red line indicates the position of Re in a low oxidation state, and the blue one indicates the position of oxidized Re, which both correspond to $4d_{5/2}$ photoelectrons. The $4d_{3/2}$ peaks are overlapped with the C1s peaks.

If we consider the real catalysts with respect to the XPS results, it is possible to argue that there is a higher amount of Re with a higher oxidation state in Ni-CuRe(7)/MS than in NiRe(7)/ MS. This might result in a higher acid activity of Ni-CuRe(7)/MS according to the observed product distribution.

The Ni2p spectra of the fresh, activated, and spent NiRe(7)/ MS and Ni-CuRe(7)/MS samples are shown in Figure 9. The fresh samples exhibited similar Ni spectra, in which is Ni mainly oxidized, but with the presence of a minor component of reduced Ni as well. After in situ H_2 activation at 623 K, Ni was reduced considerably, but not totally. Interestingly, a significant fraction of Ni was still oxidized after the in situ reduction in the Ni-CuRe(7)/MS sample (&75% of oxidized Ni). In contrast, the degree of Ni reduction was much higher in the sample without Cu, NiRe(7)/MS (&57% of oxidized Ni). This, together with the difficulty to reduce Re in the Ni-CuRe(7)/MS sample during the in situ reduction treatment, suggests that the presence of Cu that interacts strongly with both Re and Ni and that Cu prevents both Re and Ni reduction. This is likely an electron donation from Re and Ni towards Cu. Finally, the Ni spectra of the spent NiRe(7)/MS and Ni-CuRe(7)/MS samples were virtually identical to those of the corresponding fresh samples. These experiments showed that in the catalyst without Cu, NiRe(7)/ MS, there was a higher amount of reduced Ni, which in turn can be correlated with its higher propanediol selectivity.

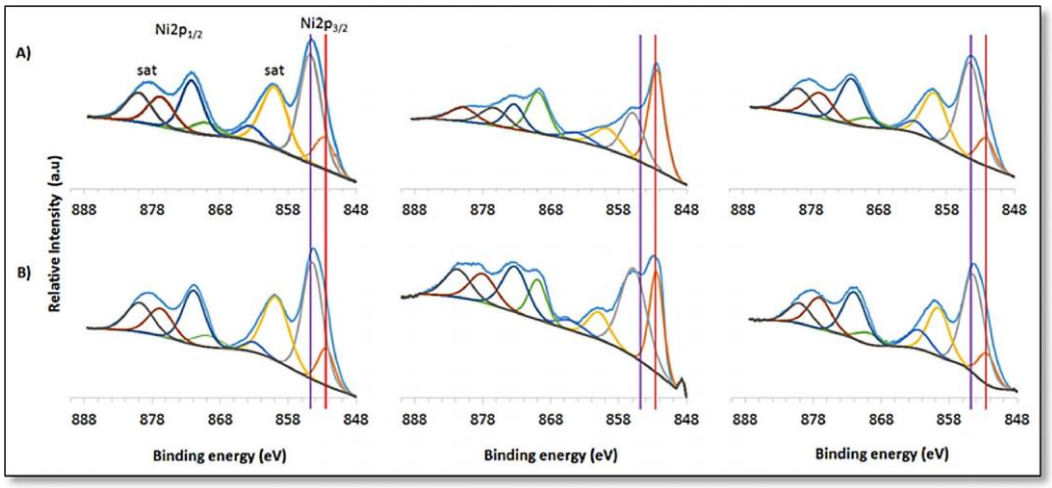

Figure 9. Ni2p XPS spectra of the fresh, H_2-activated, and spent catalysts from left to right of A) NiRe(7)/MS and B) Ni-CuRe(7)/MS. The red line indicates the position of reduced Ni, and the blue one indicates the position of oxidized Ni ($2p_{3/2}$ photoelectrons).

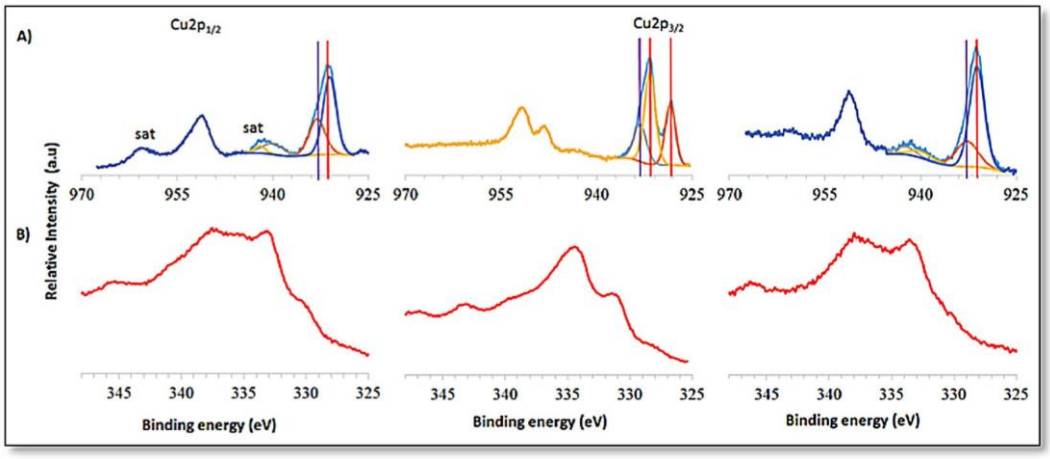

Figure 10. A) Cu2p XPS and B) Auger Cu LMM spectra of fresh, H_2-activated, and spent Ni-CuRe(7)/MS catalyst. The red line indicates the position of reduced Cu, and the blue one indicates the position of oxidized Cu ($2p_{3/2}$ photoelectrons). In addition, Cu^{II} species are accompanied by satellite lines (sat).

The Cu2p spectrum of Ni-CuRe(7)/MS and the Cu LMM Auger lines are shown in Figure 10. In the spectrum of the fresh sample both reduced and oxidized Cu can be observed. However, after in situ H_2 activation at 623 K, the spectrum changed dramatically and Cu was reduced strongly (&78%). This was also observed clearly in the Auger lines, and the peaks at 334.9 and 332.0 eV showed clearly the presence of metallic Cu. We highlight the absence of satellite lines and the appearance of two different reduced Cu species after the in situ reduction treatment in the Cu2p spectra. At this point it is difficult to identify the nature of these two species unambiguously. One of the components may correspond to metallic Cu and the other one can be assigned to a Cu–M interaction. The electron donation from Re and Ni towards Cu in the NiCuRe(7)/MS sample, discussed above, agrees with the observed strongly reduced component in the Cu2p spectrum, which is compatible with the existence of a type of Cu that acts as an electron acceptor. Finally, the spectrum of the spent sample was similar to that of the fresh one, although the lower intensity of the satellite lines in the 2p spectrum indicates a slightly higher reduction character in the spent sample.

Conclusions

Ni-Cu catalysts prepared at 40 wt% total metal loading were modified with 7 wt% Mo, V, W, and Re. Some catalysts with different Ni-Cu/Re ratios and Re-modified monometallic Ni and Cu catalysts were also prepared for comparison. The characterization results revealed that the presence of V and Mo modifiers made the reduction of NiO more difficult. The reducibility of NiO became harder if the metal loading was lower. The total surface acidity and acid strength increased in the presence of modifiers with an increase in the amount of modifier and a decrease in the metal loading. BET surface area analysis and XRD were used to confirm that the dispersion of the NiO and the Ni in the catalyst precursors and catalysts, respectively, increased in the presence of modifiers and with a decrease in the Ni-Cu loading. The dispersive effect was higher in the presence of the Re modifier.

The catalytic activity of all the modified catalysts was comparable to or higher than that of the unmodified catalysts. The presence of V and Re as modifiers increased the 1,3-propanediol (1,3-PrD) and 1,2-propanediol (1,2-PrD) ratio to 0.45 and 0.7, respectively, from that of the unmodified catalyst (0.33) or that modified with W (0.24) or Mo (0.33). The results confirmed that Re plays an important role to improve the 1,3-PrD production. The W-modified catalyst gave the highest selectivity to propanediol (82%), the lowest selectivity to condensation products (2%), and the lowest 1,3-PrD/1,2-PrD ratio, in agreement with its high NiO reducibility and hence metal activity.

The important role of the Re modifier was confirmed by the increase of the 1,3-PrD/1,2-PrD ratio if the Re/Ni+Cu ratio was increased by increasing the Re content or by decreasing the Ni-Cu loading. However, at a low metal loading the diol selectivity was low and the selectivity to the condensation products was high as would be expected from the low NiO reducibility and high acidity of these samples. The monometallic Cu catalysts gave the lowest propanediol and the highest condensation products selectivity comparable to that of the Re-modified support without an active metal. This confirmed the lower hydrogenolysis capacity of Cu in the catalytic system. The Remodified Ni catalysts showed a high 1,3-PrD/1,2-PrD ratio (1.24), a high propanediol selectivity, and the highest 1,3-PrD yield (46.1%) of all the catalysts studied. These results can be explained by some decoration of the Ni particles by the ReO_x, as can be deduced from the X-ray photoelectron spectroscopy results, which favor the collaborative action between the metal sites and ReO_x responsible for the 1,3-PrD production. The yield of 1,3-PrD obtained in this work was comparable to or higher than that reported previously for the hydrogenolysis of glycerol using noble-metal catalysts under harsh reaction conditions and with long reaction times.

Experimental Section

Preparation of supported catalysts

Mesoporous saponite in the H^+ form (MS; surface acidity, 1.02 $mEq._{H+}g^{-1}$) synthesized as reported previously[19] was used as a support for catalyst preparation. MS was stable until 1035 K (temperature of clay dehydroxylation), which was determined by using TGA.[19] Ni-Cu/MS catalysts with 20, 30, and 40 wt% total metal loading and a Ni/Cu ratio of 6:1 were prepared by the impregnation of 1 g of the support with a calculated volume of 0.5m Ni-Cu in ethanol solution that contained appropriate amounts of $Ni(NO_3)_2$ and $Cu(NO_3)_2$. After the solvent was removed by rotary evaporation and drying at 383 K overnight, the samples were calcined at 723 K for 5 h.

Several Ni-Cu-MO_x/MS (M=W, Mo, V and Re) catalysts were prepared by impregnating the Ni-Cu/MS (prepared at 40 wt% Ni-Cu loading) with an aqueous solution of the modifier metal precursors, $(NH_4)_{10}W_{12}O_{41}{\cdot}4H_2O$, $(NH_4)_6Mo_7O_{24}{\cdot}4H_2O$, NH_4VO_3, and NH_4ReO_4. The amount of MO_x modifier expressed per mass of W, Mo, and V with respect to the unmodified catalyst was 7 wt%. The Re loading was varied at 3, 7, and 15 wt% to result in the catalysts Ni-CuRe(3)/MS, Ni-CuRe(7)/MS, and Ni-CuRe(15)/MS with M/Re molar ratios of 42, 18, and 8, respectively.

The effect of the Ni-Cu/Re ratio was also studied by decreasing the metal loading at 30 and 20 wt% Ni-Cu and maintaining the Re loading as in the Ni-CuRe(7)/MS catalyst. This was performed to increase the acid contribution of the support by decreasing the support acid site coverage. The resulting catalysts were labeled NiCu*Re(7)/MS and Ni-Cu**Re(7)/MS for 30 and 20% metal loading, respectively. The (Ni+Cu)/Re molar ratios for these catalysts were 13 and 9. Monometallic Ni and Cu catalysts were prepared at 40 wt% metal loading and modified with 7 wt% Re for comparison.

All catalysts were reduced by using a tubular reactor under H_2 flow (75 $mLmin_{@}^{1}$) at 623 K for 6 h. The catalyst precursors were labeled with P at the beginning of the name. The nomenclature, type of modifier, and amount of metal and modifier loading of the catalysts are listed in Table 4.

Table 4. Nomenclature, type of modifier, amount of metal, and modifier loading of the catalysts.

Catalysts	Total Ni-Cu [wt%]	Modifier M (MO_x)	Modifier [wt%]
Ni-Cu/MS	40	–	–
Ni-CuV(7)/MS	40	V	7
Ni-CuMo(7)/MS	40	Mo	7
Ni-CuW(7)/MS	40	W	7
Ni-CuRe(7)/MS	40	Re	7
Ni-CuRe(3)MS	40	Re	3
Ni-CuRe(15)/MS	40	Re	15
Ni-Cu*Re(7)/MS	30	Re	7
Ni-Cu**Re(7)/MS	20	Re	7
NiRe(7)/MS	40	Re	7
CuRe(7)/MS	40	Re	7

Catalysts characterization

XRD patterns of powdered catalyst samples were recorded by using a Siemens D5000 diffractometer equipped with CuK_a radiation (l=1.54 a) source. Measurements were performed at 2q=5– 708 with an angular step of 0.058 and at a rate of 3 s per step. Crystalline phases were identified by comparison of the diffractogram of the sample with reference data from the International Centre for Diffraction Data (JCPDS files). Integral breadth estimated by fitting intense reflection peaks of metal or metal oxide particles and by applying TOPAS 4.1 was used to calculate the crystallite sizes using the Scherrer equation.

N_2 adsorption–desorption analysis was performed by using a Quadrasorb sorptometer at 77 K to determine the specific BET area and porosity. Before measurement, samples (&0.1 g) were degassed overnight at 383 K. The specific surface area was determined by applying the BET method, and the pore size distribution was estimated by the Barrett–Joyner–Halenda (BJH) method.

TEM characterization was performed by using a JEOL 1011 transmission electron microscope operated at an accelerating voltage of 100 kV and magnification of 200 k. The sample (0.1 mg) was dispersed in ethanol (50 mL) by using an ultrasonic bath. Then it was deposited on a carbon-coated copper grid and air dried.

TPR of the catalyst precursors was measured by using an Autochem AC2920 Micrometric apparatus. The catalyst precursor sample, calcined beforehand (0.1 g), was placed in a tubular reactor and heated between RT and 1173 K at a rate of 10 $Kmin_{@}^{1}$ under a flow of 5 vol% H_2 in argon (50 $mLmin_{@}^{1}$). The H_2 consumption was recorded by using a thermal conductivity detector (TCD).

The total surface acidity of the catalyst precursors was determined by using TGA of CHA-treated samples (&0.1 g) following the protocol described by Mokaya et al.[21] The analysis was conducted by using a Labsys Setaram TGA microbalance equipped with a programmable temperature furnace. Each sample was heated under a N_2 flow (80 $cm^3 min_{@}^{1}$) from 303 to 1173 K at a rate of 5 $Kmin_{@}^{1}$. The total acidity was equivalent to the amount of CHA desorbed in the temperature range of 523–923 K in which the sample without CHA treatment did not show any significant mass loss.[19]

Several NH_3-TPD experiments were performed on selected catalyst precursors to complement the acidity results obtained by using CHA-TGA analysis and to compare the relative contribution of external and internal acid sites. The analysis was conducted by using an AC2920 apparatus. Typically, approximately 0.2 g of sieved catalyst precursor was loaded into a U-shaped quartz tube and submitted to surface pretreatment under a flow of He at 623 K for 1 h. It was then cooled to 373 K and saturated with pure NH_3 for 30 min. The physically adsorbed NH_3 was removed by purging the sample with pure He for 30 min, the sample was heated from 373 to 973 K at a heating rate of 10 Kmin@1, the NH_3 desorption was monitored by using a TCD. The peak area of the detected TPD peak was correlated to the amount of desorbed NH_3 from a pulsed NH_3 injection experiment, and the total surface acidity was predicted from the amount of ammonia desorbed.

Surface characterization of some fresh, spent, and H_2 in situ activated catalysts was performed by using XPS by using a SPECS system equipped with an Al anode XR50 source operated at 150 mW and a Phoibos MCD-9 detector. The pressure in the analysis chamber was kept below 10@7 Pa. The area analyzed was approximately 2 mmV2 mm. The pass energy of the hemispherical analyzer was set at 25 eV, and the energy step was fixed at 0.1 eV. Powdered samples were pressed to self-supported pellets. In situ experiments were performed under dynamic conditions in an adjacent chamber at atmospheric pressure equipped with a mass spectrometer and an IR lamp to heat the sample. The sample was transferred under ultra-high vacuum between the in situ chamber and the analysis chamber. Gases were dosed accurately into the in situ chamber by using mass flow controllers, and the temperature was measured by using a K-type thermocouple in contact with the sample holder. Data processing was performed with the CasaXPS program (Casa Software Ltd., UK). The BE values were referenced to the C1s peak at BE=284.8 eV. Atomic fractions were calculated using peak areas normalized from the acquisition parameters after background subtraction, experimental sensitivity factors, and transmission factors provided by the manufacturer.

Catalytic activity test

The activity test was performed in a 50 mL stainless-steel autoclave equipped with an electronic temperature controller and a mechanical stirrer. Glycidol (3.77 mL) was dissolved in sulfolane (30 mL) and purged with N_2, and 1 g of freshly reduced catalyst was transferred carefully into the reactor under a positive N_2 pressure to avoid contact with the atmosphere. The reactor was sealed, purged three times with 4 MPa N_2 and three times with 1 MPa H_2. After a leakage test was performed, the temperature of the reaction was set at 393 K. The reaction mixture was stirred vigorously at 600 rpm. Together with the use of powdered catalysts and the mesoporous nature of the support used for catalyst preparation, this avoids internal and external mass and heat transfer limitations and diffusion problems. Once the temperature on the electronic control read the final temperature of the reaction, the H_2 pressure was adjusted to 5 MPa and the reaction time was started (t_0). The reaction was run for 4 h, and H_2 was fed on demand. At the end of the reaction (t_f), the mixture was cooled, and the reaction products were separated from the catalyst by filtration. The liquid products were analyzed by using a Shimadzu GC-2010 chromatograph using a SupraWAX-280 capillary column, 1-butanol as internal standard, and a flame ionization detector (FID).

Acknowledgements

The authors are grateful for the financial support of the Ministerio de Econom&a y Competitividad of Spain and FEDER funds (CTQ2011-24610). J. Llorca is Serra Hfflnter Fellow and is grateful to ICREA Academia program.

[1] a) M. Schlaf, Dalton Trans. 2006, 4645–4653; b) A. Corma, S. Iborra, A. Velty, Chem. Rev. 2007, 107, 2411–2502; c) P. C. A. Bruijnincx, Y. Rom#nLeshkov, Catal. Sci. Technol. 2014, 4, 2180–2181.

[2] C.-H. Zhou, J. N. Beltramini, Y.-X. Fan, G. Q. Lu, Chem. Soc. Rev. 2008, 37, 527–549.

[3] a) R. M. West, E. L. Kunkes, D. A. Simonetti, J. A. Dumesic, Catal. Today 2009, 147, 115–125; b) A. Yamaguchi, N. Hiyoshi, O. Sato, K. K. Bando, M. Shirai, Green Chem. 2009, 11, 48–52.

[4] a) Y. Nakagawa, K. Tomishige, Catal. Sci. Technol. 2011, 1, 179–190; b) S. Sitthisa, T. Sooknoi, Y. Ma, P. B. Balbuena, D. E. Resasco, J. Catal. 2011, 277, 1–13; c) K. L. Deutsch, B. H. Shanks, J. Catal. 2012, 285, 235–241.

[5] a) P. M-ki-Arvela, J. H#jek, T. Salmi, D. Y. Murzin, Appl. Catal. A 2005, 292, 1–49; b) Y. Nakagawa, M. Tamura, K. Tomishige, J. Mater. Chem. A 2014, 2, 6688–6702.

[6] a) M. A. Dasari, P.-P. Kiatsimkul, W. R. Sutterlin, G. J. Suppes, Appl. Catal. A 2005, 281, 225–231; b) Y. Kusunoki, T. Miyazawa, K. Kunimori, K. Tomishige, Catal. Commun. 2005, 6, 645–649; c) T. Miyazawa, S. Koso, K. Kunimori, K. Tomishige, Appl. Catal. A 2007, 329, 30–35; d) J. Feng, J. Wang, Y. Zhou, H. Fu, H. Chen, X. Li, Chem. Lett. 2007, 36, 1274–1275; e) T. S#nchez, P. Salagre, Y. Cesteros, A. B. Ljpez, Chem. Eng. J. 2012, 179, 302–311.

[7] a) P. N. Caley, R. C. Everett (DuPont), Patent US 3350871, 1967; b) D. Zimmerman, R. B. Isaacson (Celanese Corp), Patent US 3814725, 1974. [8] A. Perosa, P. Tundo, Ind. Eng. Chem. Res. 2005, 44, 8535–8537.

[9] a) T. Kurosaka, H. Maruyama, I. Naribayashi, Y. Sasaki, Catal. Commun. 2008, 9, 1360–1363; b) J. Chaminand, L. Djakovitch, P. Gallezot, P. Marion, C. Pinel, C. Rosier, Green Chem. 2004, 6, 359–361; c) N. Suzuki, Y. Yoshikawa, M. Takahashi, M. Tamura (KAO Corporation), World Pat. 2007129560, 2007; d) E. I. Ross-Medgaarden, W. V. Knowles, T. Kim, M. S. Wong, W. Zhou, C. J. Kiely, I. E. Wachs, J. Catal. 2008, 256, 108–125; e) L. Liu, Y. Zhang, A. Wang, T. Zhang, Chin. J. Catal. 2012, 33, 1257–1261; f) J. ten Dam, K. Djanashvili, F. Kapteijn, U. Hanefeld, ChemCatChem 2013, 5, 497–505; g) R. Arundhathi, T. Mizugaki, T. Mitsudome, K. Jitsukawa, K. Kaneda, ChemSusChem 2013, 6, 1345–1347; h) S. Zhu, X. Gao, Y. Zhu, Y. Li, J. Mol. Catal. A 2015, 398, 391–398; i) S. Zhu, Y. Qiu, Y. Zhu, S. Hao, H. Zheng, Y. Li, Catal. Today 2013, 212, 120–126; j) S. Zhu, X. Gao, Y. Zhu, J. Cui, H. Zheng, Y. Li, Appl. Catal. B 2014, 158–159, 391– 399.

[10] L. Gong, Y. Lu, Y. Ding, R. Lin, J. Li, W. Dong, T. Wang, W. Chen, Appl. Catal. A 2010, 390, 119–126.

[11] M. Chia, Y. J. Pag#n-Torres, D. Hibbitts, Q. Tan, H. N. Pham, A. K. Datye, M. Neurock, R. J. Davis, J. A. Dumesic, J. Am. Chem. Soc. 2011, 133, 12675–12689.

[12] Y. Nakagawa, Y. Shinmi, S. Koso, K. Tomishige, J. Catal. 2010, 272, 191– 194.

[13] K. Chen, S. Koso, T. Kubota, Y. Nakagawa, K. Tomishige, ChemCatChem 2010, 2, 547–555.

[14] a) W. Yoo, Z. Mouloungui, A. Gaset, USP 6316641, 2001; b) R. Bai, H. Zhang, F. Mei, S. Wang, T. Li, Y. Gu, G. Li, Green Chem. 2013, 15, 2929– 2934.

[15] K. Chen, K. Mori, H. Watanabe, Y. Nakagawa, K. Tomishige, J. Catal. 2012, 294, 171–183.
[16] S. Liu, Y. Amada, M. Tamura, Y. Nakagawa, K. Tomishige, Green Chem. 2014, 16, 617–626.
[17] a) S. Koso, N. Ueda, Y. Shinmi, K. Okumura, T. Kizuka, K. Tomishige, J. Catal. 2009, 267, 89–92; b) S. Koso, H. Watanabe, K. Okumura, Y. Nakagawa, K. Tomishige, Appl. Catal. B 2012, 111–112, 27–37.
[18] F. B. Gebretsadik, J. Ruiz-Martinez, P. Salagre, Y. Cesteros, Appl. Catal. A, https://doi.org/10.1016/j.apcata.2017.03.018.
[19] F. B. Gebretsadik, D. Mance, M. Baldus, P. Salagre, Y. Cesteros, Appl. Clay Sci. 2015, 114, 20–30.
[20] M. Bartjk, A. F#si, F. Notheisz, J. Catal. 1998, 175, 40–47.
[21] R. Mokaya, W. Jones, S. Moreno, G. Poncelet, Catal. Lett. 1997, 49, 87–
94.